

## Influence of Rapid Cooling of Copper Oxide Nanostructures Synthesized Via Thermal Oxidation of Copper Foil

**Dr. Abdulqader D. Faisal**

Applied Sciences Department, University of Technology /Baghdad

Email:abdulf330@gmail.com

**Dr. Wafaa Khalid Khalef**

Applied Sciences Department, University of Technology /Baghdad

Email: drwafaa1980@gmail.com

**Haitham Talib Hussein**

Applied Sciences Department, University of Technology /Baghdad

Email: haitham.tumy@yahoo.com

Received on:3/3/2016 & Accepted on:20/10/2016

### ABSTRACT

The influence of rapid cooling on the morphology and structures of CuO nanostructures synthesized via oxidation process was investigated. Two suggested approaches were used in this study. First and second oxidation approaches of Cu foil were conducted with single zone tube furnace and muffle furnace respectively. The copper oxide product was characterized with X-ray diffraction (XRD), scanning electron microscope (SEM), Fourier transform –infrared spectrometer (FTIR), ultra violet- visible (UV-VIS) spectrophotometer. XRD patterns showed that there are two copper oxide phases of Cu<sub>2</sub>O and CuO always coexists and their intensity proportion varying with oxidation temperatures. These results were confirmed by SEM and FTIR analysis. High energy band gap about 3.6eV was calculated at different temperatures for copper oxide nanostructure.

**Keywords:** thermal oxidation; copper oxide; rapid cooling; crystal structure; nanostructure materials

### INTRODUCTION

Copper Oxide is a p-type semiconductor oxide that is being widely studied due to its interesting properties and applications. Cupric oxide (CuO) having a band gap of 1.21–1.51 eV and monoclinic crystal structure and cuprous oxide (Cu<sub>2</sub>O) having a band gap of approximately 2.0 eV and a cubic crystal structure [1]. Its high optical absorption coefficient in the visible range and reasonably good electrical properties constitute important advantages and render Cu<sub>2</sub>O as the most interesting phase of copper oxides [2]. Copper oxides nanostructures have been synthesized by using various methods like: chemical spray pyrolysis [3], DC sputtering [4], thermal oxidation [5]; electro deposition [6]; chemical deposition [7]; wet chemical [8]; spraying [9]; chemical vapor deposition [10]; plasma evaporation [11]; reactive sputtering [12]; and molecular beam epitaxy [13]. However, all these methods either require high temperatures, sophisticated instrumentation, inert atmosphere, or long reaction time. Among these methods, thermal oxidations of Cu metal in air represent low cost method, long time and moderate temperature. The formation of cupric oxide nanowires (CuO NW's) by direct thermal oxidation of metals has been recently given considerable attention due to its simplicity and large-scale growth capability [5]. Oxide NWs prepared by thermal oxidation exhibit higher crystallinity and high aspect ratios compared to those prepared via solution-based routes [5, 14]. The thermal oxidation technique can be used to fabricate nanowires that are low cost and high quality. A growth condition can be controlled with difference temperature and time. In most of these studies, a mixture of phases of Cu, CuO and Cu<sub>2</sub>O is generally obtained and this is one of the nagging problems for non-utilizing Cu<sub>2</sub>O as a semiconductor. Pure Cu<sub>2</sub>O films can be

obtained by oxidation of copper layers within a range of temperatures followed by annealing for a small period of time [14]. In the present work, new approaches were presented to investigate the influence of rapid cooling on copper oxide nanostructures synthesized via thermal oxidation of copper foil. Where copper sheets oxidized in static air at different temperatures followed by rapid cooling to produces copper oxide nanostructure. Structure, morphology, composition of these films were determined with X-rays diffraction (XRD), scanning electron microscope (SEM) and Fourier transform infrared (FTIR) spectroscopy in transmitted mode respectively. The optical properties of the thin films were also studied with UV-Visible spectrophotometer.

### Experimental

Sheet of commercial grade copper foil was cut into pieces with equal sizes of 25mmx10mmx0.1mm. These were subsequently washed with detergent solution, demonized water, and then sonicated with acetone and ethanol for 15 minute each, rinsed with deionized water and dried with stream of nitrogen gas. Two oxidation approaches of oxidation experiments were conducted at two different furnaces. First oxidation approach was conducted in homemade single zone tube furnace with open sides quartz tube(3cm diameter,100cm long) working at heating rate of 40°C/minutes at air. The cleaned of copper foils were loaded on alumina boat and inserted into the middle of the quartz tube. The foils were heated to temperatures of 500°C, 550°C and 650°C in air for 1h. After oxidation reaction by heating, the copper plate was immediately taken out from the furnace and cooled down in air in order to cool down rapidly to room temperature. Second oxidation approach was conducted in programmable muffle furnace (Nabertherm, Germany) working at heating rate of 20°C/minutes.

### Characterization

The crystalline structure of the product was confirmed by using x-ray diffraction. This analysis was done with Shimadzu XRD – 6000/Japan, diffractometer equipped with Cu K<sub>α</sub> radiation ( $\lambda=1.5406\text{\AA}$ ) employing a scanning rate of and  $2\theta$  ranges from  $20^{\circ}$ -  $60^{\circ}$ . The morphology of the product was observed with scanning electron microscope - SEM (Tescan Vega II- Cheek). The FTIR transmissionspectrum in the range of 400-4000  $\text{cm}^{-1}$  was recorded using Shimadzu – ARAffinity-1/ Japan. The optical transmittance of the CuO was measured using spectrophotometer (UV-visible-2450 spectrophotometer, Shimadzu).

### Results and Discussion:

First oxidation approach (Tube Furnace)

#### SEM morphology analysis

The morphology of copper foil oxidized in static air at various temperatures of 550°C, 600°C and 650°C for one hour using tube furnace was investigated by SEM. The oxidation results are shown in Fig.1. Figure 1a show the small amount of CuO nanowires grown at 550°C, which is confirmed by XRD in Fig. 2a. Different morphology at temperature 600°C is shown in Fig. 1b. It can be observed that the shapes of these crystals are rounded with large size. These round shape crystals can be attributed to the melting process effect. It was seen from the present work that heating and rapid cooling process leads to produce mainly Cu<sub>2</sub>O phase mixed with small amount of CuO. The oxidation of copper foil at 600 °C shows a continuous and homogeneous granular surface as observed in Fig.1b. While for copper foil oxidized at 650°C showed dense and semi spherical structures with grain size increases with increasing oxidation temperature as shown in Fig. 1c. This result is in a good agreement with XRD results presented in Fig.2b.

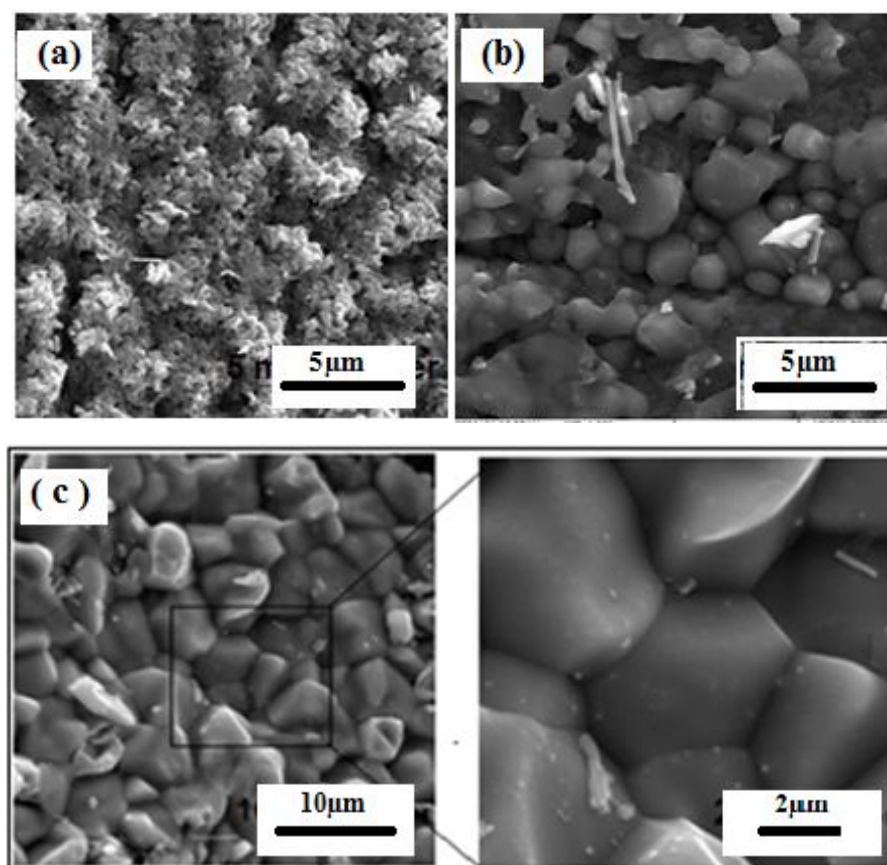


Figure (1).SEM images of Cu foil oxidized in static air at (a) 550°C, (b) 600°C and (c) 650°C for 1h in air.

#### XRD structural analysis

Figure 2 shows the XRD pattern of copper oxide produced by thermal oxidation at different temperatures (550°C and 650°C) followed by rapid cooling of oxidized copper sheets. The material was scanned in the range of  $20^\circ - 60^\circ$ . The XRD pattern in Fig.2a represent the oxidation temperature at 550°C shows the presence of peaks at  $29.66^\circ$ ,  $35.66^\circ$ ,  $36.52^\circ$ ,  $38.79^\circ$ , and  $42.38^\circ$ . Another peaks with small intensities near to  $2\theta = 35.66^\circ$  and  $38.79^\circ$  which match reflections from the (002) and (111) planes for CuO respectively, while the other peaks at  $29.66^\circ$ ,  $36.52^\circ$  and  $42.38^\circ$  are belongs to (110), (111) and (200) planes of  $\text{Cu}_2\text{O}$  respectively. The pattern in Fig. 2b represent the oxidation at temperature of 650°C is quite similar to the one in Fig.1a but the peak of  $\text{Cu}_2\text{O}$  (200) disappear due to the high temperature conversion. These are in good agreement with the standards of the joint committee on powder diffraction standards JCPDS card #05-667 for  $\text{Cu}_2\text{O}$  and Card # 05-661 for CuO. No traces of Cu metal and any other impurities were detected. This means that the copper foil was converted subsequently to  $\text{Cu}_2\text{O}$ , CuO layers and then to CuO nanowires at these oxidation temperatures. The conversion is reported to take place at temperatures above  $400^\circ\text{C}$  [15].Thermal oxidation followed by rapid cooling produces almost  $\text{Cu}_2\text{O}$  (111) with very small amount of CuO phase.

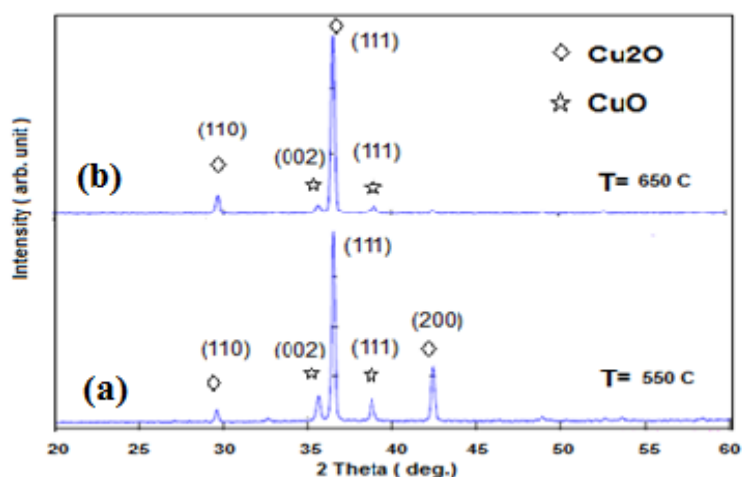


Figure (2).XRD pattern of copper foil oxidized in air at 550°C (a) and 650°C (b)for 1h.

The lattice parameter for Cu<sub>2</sub>O strongest reflection (111) was calculated from the relation [16]:  $d = a_0 / (h^2+k^2+l^2)^{1/2}$  [for cubic structure] (1)

The d-values (inter-planer spacing) was calculated from Bragg's law, and a<sub>0</sub> is the lattice parameter. The calculated lattice parameters of Cu<sub>2</sub>O (111) products are shown in Table 1.The crystallite size was calculated by the x-ray line broadening method using the Scherrer formula [17]:

$$L = k \lambda / \beta \cos\theta \tag{2}$$

Where L is the crystallite size (or particle size) to be calculated, k is the Scherrer constant,  $\lambda = 1.5406\text{\AA}$  is the wave length of radiation used Cu k<sub>α</sub>, β is calculated from full width half maximum (FWHM) for the strongest diffraction peak, and θ is the diffraction angle of the concerned diffraction peak. Assuming that k = 0.9 which corresponds to spherical crystallites. The particle size of Cu<sub>2</sub>O was calculated using Scherrer formula for the strongest peak at(111) reflection plane for both XRD pattern shown in Fig. 2. The calculated crystallite size of Cu<sub>2</sub>O (111) product are shown in Table 1. The average values of the crystallite size of copper oxide were calculated within around 39 nm as the oxidation temperature increased from 550°C to 650°C.The average crystal size value gives an indication that the copper oxide prepared is Nano crystalline in nature.

Table (1) The calculated lattice parameter a<sub>0</sub>(Å) and crystallite size L (nm) for Cu<sub>2</sub>O and CuO.

Present work							Standard Data
Oxidation temp.(°C)	2θ°	d <sub>(111)</sub> (Å)	Phase (plane)	a <sub>0</sub> (Å)	FWHM°	L(nm)	
550	36.50 27	2.45956	Cu <sub>2</sub> O (111)	4.26008	0.26480	36	Cu <sub>2</sub> O : JCDPS File # 05-0667  and
	42.38 24	2,13095	Cu <sub>2</sub> O (200)	4.2619	0.25750	44	
650	36.51 61	2.45869	Cu <sub>2</sub> O (111)	4.25857	0.22550	38	CuO : JCDPS File # 05-0661

### FTIR Analysis

In order to record infrared pattern, the copper oxide product was removed from the foil by scraping. The scraped material was grinded to a fine powder using small mortar. The grinded oxide powder was mixed with KBr powder then a pellet was prepared for FTIR test. Typical FTIR transmission spectrum of copper oxide annealed at 650°C only is shown in Fig. 3. This spectrum show strong peak at 621 $\text{cm}^{-1}$  corresponding to the vibrational mode of CuO in Cu<sub>2</sub>O phase. In addition, weak absorption peaks at 427  $\text{cm}^{-1}$  and 420  $\text{cm}^{-1}$  are related to the vibrational modes in Cu-O phase. These results are in agreement with XRD results previously discussed (Fig.2b). Another peak at 3452  $\text{cm}^{-1}$  is due to O-H stretching bond as a result of water through washing process. Our results are in a good agreement with other workers results [18, 19].

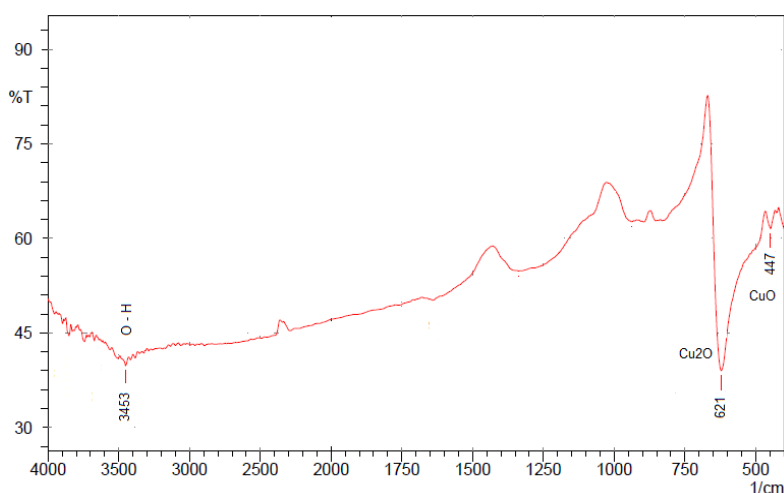


Figure (3) FTIR transmission spectrum of copper oxide thermally annealed at 650°C for 1h.

### Second oxidation approaches (Muffle Furnace)

#### SEM morphology analysis

The morphologies of as synthesized CuO products were observed by scanning electron microscope (SEM) as explained in Figs.(4, 5, and 6) at various magnifications. Fig.4 shows SEM images for CuO NWS synthesized by oxidation of Cu foil in static air at 550°C for 1h, followed by rapid cooling. There are long CuO nanowires with estimated length and diameter of about 20 $\mu\text{m}$  and 100nm respectively. Other small nanowires starts to grow at different area as shown in Figures 4b,4c, and 4d. The circle in Fig.4a represents a magnified area as presented in Figs, 4b, 4c, and 4d. The length of CuO wires could grow longer if the oxidation time set for longer. The presence of CuO nanowires was confirmed by XRD analysis shown in Fig. 7a. Another oxidation process was carried out at temperatures of 600°C and 650°C for 1h in static air as shown from SEM in Figs.5 and 6 respectively. Mixed phases of Cu<sub>2</sub>O and CuO phases are found in Fig.5 and Fig.6 as confirmed by XRD analysis. Different morphology of the crystal can be seen in Fig.5 which is attributed to CuO crystal deformation to CuO nanowires as clearly shown as protrudes on the crystals referred by circles in Fig5c and Fig.5d. The average size of these crystals are in the range of 200-400nm. It is indicated that the CuO nanowires on top most layer is just starts to grow from these crystals at this temperature. Nano crystals of CuO are growing at top most layers at higher temperature of 650°C as shown in Fig. 6. The shape is look like pyramid Nano crystals with average size of 100-300nm. These sizes of the crystals are quite small compared with micrometer sizes of the crystals obtained previously using tube furnace oxidation approach. So, it could be concluded that the scanning electron microscope results for both processes of Cu foil oxidation shows different results. This may be due to the accurate and controllable heating process with the programmable muffle furnace.

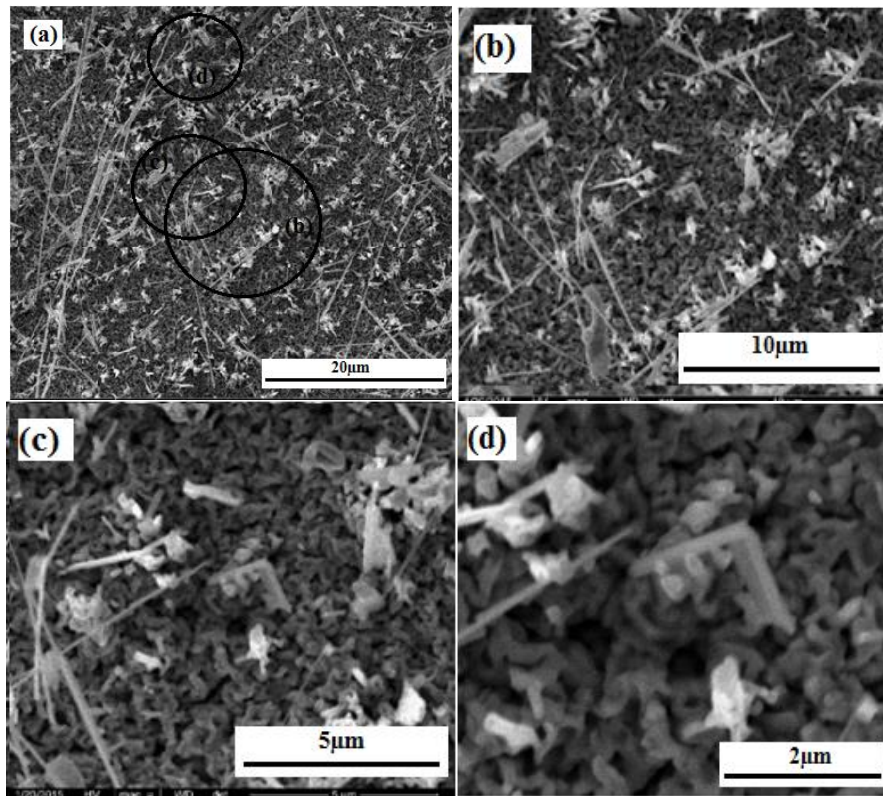


Figure (4) SEM images at various magnifications for CuO NWs grown by oxidation of Cu foil in static air at 550°C for 1h, followed by rapid cooling

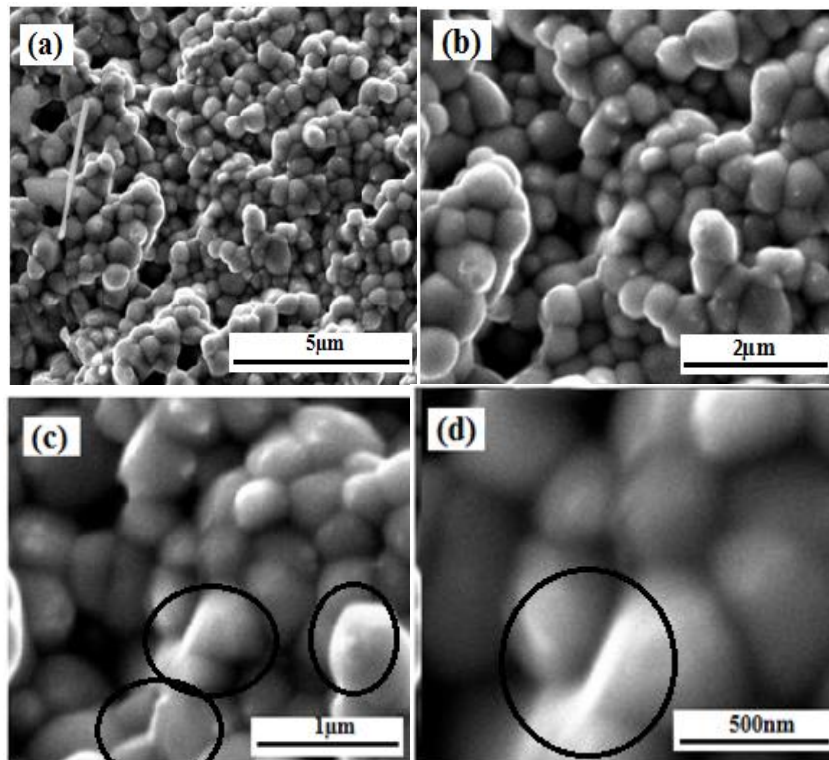


Figure (5) SEM images for copper oxide crystals synthesized by oxidation of Cu foil in static air at 600°C for 1h, followed by rapid cooling. (Crystal size = 100-300nm).

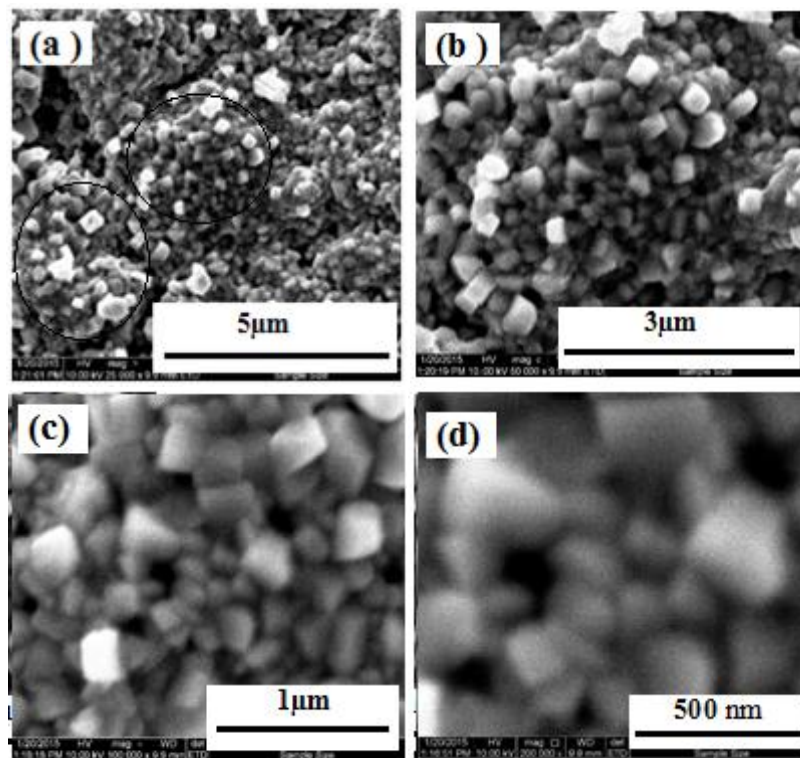
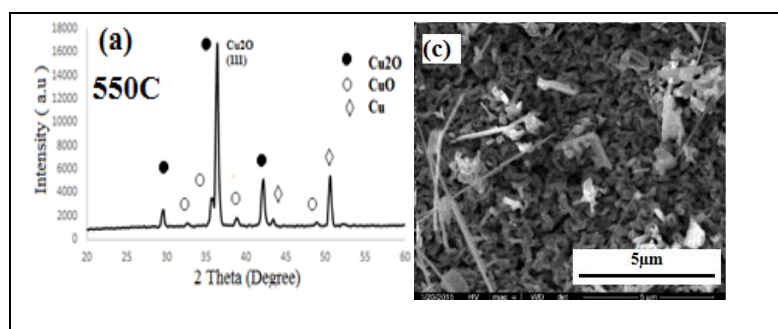
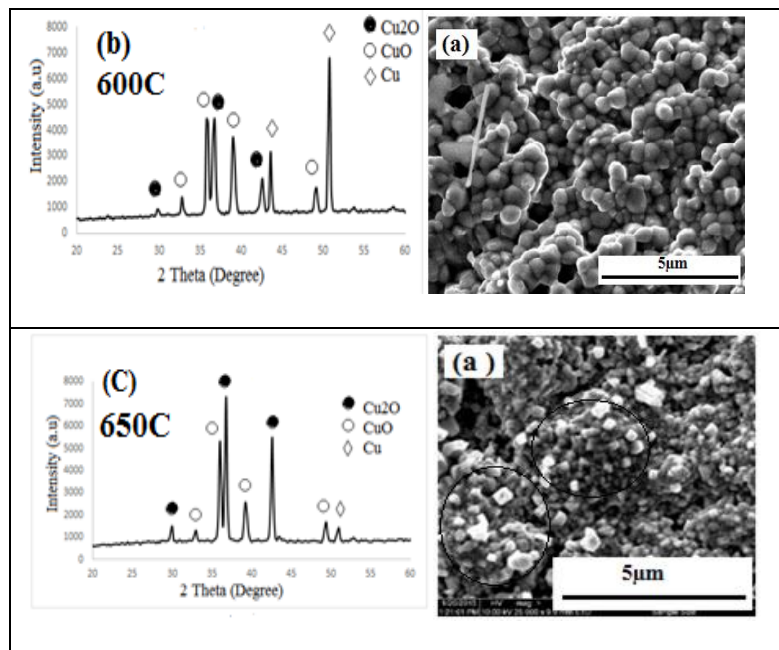


Figure (6) SEM images at various magnifications for copper oxide crystals synthesized by oxidation of Cu foil in static air at 650°C for 1h, followed by rapid cooling.(Crystal size 100-300nm).

### Restructure analysis

Figure 7 a ,b and c represents the XRD pattern and the corresponding SEM images (on left for the three samples) of copper foil oxidized at 550°C, 600°C, and 650°C for 1h in muffle furnace at static air respectively. There are always three mixed phases of Cu, Cu<sub>2</sub>O, and CuO presents in these XRD pattern. These phases are varies in quantity, it depends on the oxidation temperature process. Fig.7a show the strong peak of Cu<sub>2</sub>O and small peaks of CuO .The copper was converted into the Cu<sub>2</sub>O and CuO with nanowires at temperature of 550°C only. The peak of CuO became strong at higher temperature of 600°C while the intensity of Cu<sub>2</sub>O peak is decreased and became comparable as shown in Fig.7b. This indicating the transformation of Cu<sub>2</sub>O to CuO Nano crystals. Moreover, both phases are present as Nano crystals with higher intensities dominated by Cu<sub>2</sub>O phase at temperature of 650°C as shown in Fig.7c. The XRD analysis was confirmed that the pure Cu foil had partially transformed into the Cu<sub>2</sub>O and CuO and contained CuO nanowires at 550°C only while at other temperatures there are two types' of Nano crystals.





Figure(7).XRD pattern and the corresponding SEM image of copper foil thermally oxidized in static air at 550°C (a), 600°C (b) and 650°C (c)for 1h followed by rapid cooling.

### Optical properties

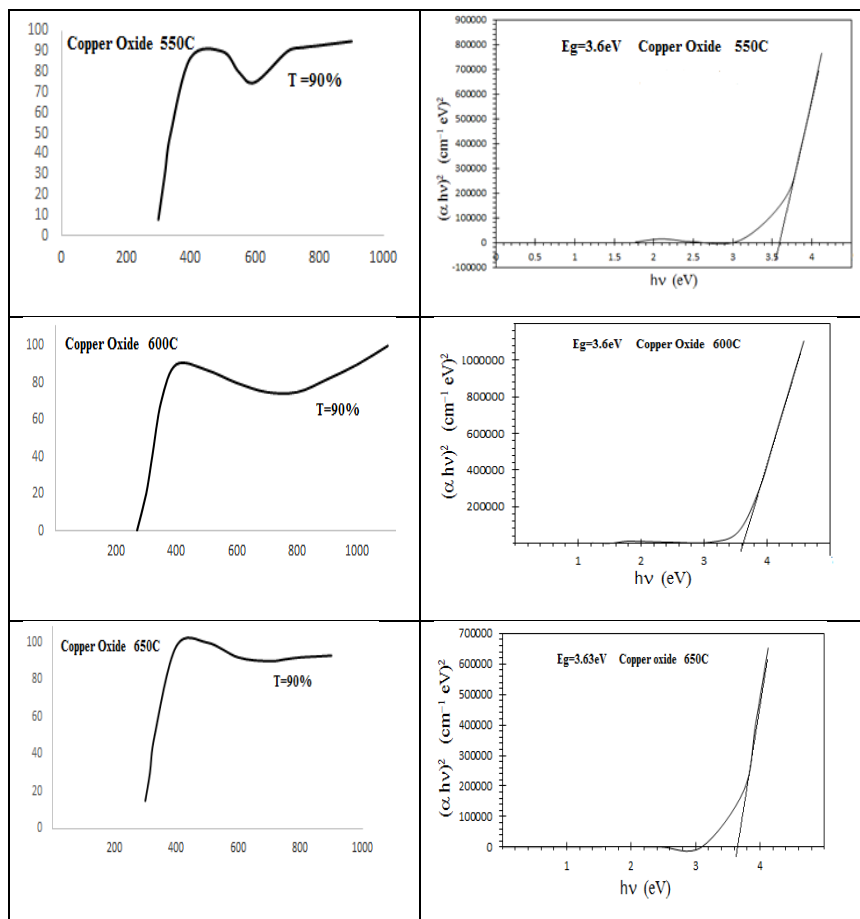
Figure 8 illustrates the UV-Visible transmittance spectra for copper oxide nanostructures in the wavelength range of 190-1100 nm. It's clear from this figure that the optical transmittance for all copper oxide samples are above 90% in the visible and NIR regions and increases with increases wavelength. Also, the transmittance spectra exhibits an intense peak centered at ~ 300 nm and another peak with lower intensity located at ~ 600 nm as shows. The peak at ~ 300 nm is due to inter band transition of copper electron from deep level of valence band while peak at ~ 600 nm is due to inter-band transition of copper electron from upper level of valence band, which is also known as surface Plasmon resonance (SPR) peak. These are an agreement results with previously reported elsewhere [18]. The optical band gap ( $E_g$ ) of a semiconductor is related to the optical absorption coefficient ( $\alpha$ ) and the incident photon energy ( $h\nu$ ) by [21]:

$$(\alpha h\nu) = (E_g - h\nu)^n \tag{3}$$

Where: n depends on the kind of optical transition. Specifically, n is 1/2 and 2 when the transition is directly and indirectly allowed, respectively. The optical band gap can be obtained by plotting the optical absorption versus the photon energy and extrapolating the linear portion of the curve to  $(\alpha h\nu)^2 = 0$ . Figure 8 show the variation of  $(\alpha h\nu)^2$  vs. photon energy ( $h\nu$ ) for copper oxide nanostructure. It's clear from figure, the optical gap of copper oxide nanostructure for all oxidation temperatures ( 550°C, 600°C and 650°C) found to be 3.6eV which is higher as compared to the bulk value of  $Cu_2O = 2.0$  eV [1]. There is an agreement with the copper oxide quantum dots results reported elsewhere [22,23]. It was reported that the band gap of semiconductor materials will increase with the decrease in particle size, which leads to blue shift in the direct band gap as a consequence of the quantum confinement effects [24]. Also the shift of the exciton peak with particle size is attributed to quantum confinement due to induced energy gap variation [25]. The spectral properties of semiconductor have been shown to vary with quantization effects. The value of band gap energy ( $\Delta E$ ) varies with the radius of the particles (d) [25]:

$$\Delta E = \left( \frac{\hbar}{2(m_e)^*} \right) \left( \frac{\pi^2}{d^2} \right) \tag{4}$$

Where  $\Delta E$  (energy shift or optical gap shift) with the respect to bulk band gap ( $\text{CuO}$ ) =1.21 eV and  $\text{Cu}_2\text{O}$ =2.0 eV) and  $d$  is the particle size,  $h$  the Planck's constant and  $(m_e)^*$  is the electron reduced mass thus with a decrease in particle size, the energy of optical transmission increases.



Figure(8).Optical properties calculation curves for copper oxide nanostructure as prepared via thermal oxidation of Cu foil at 550°C (a) 600°C (b) and 650°C , followed by rapid cooling.

## CONCLUSION

In the present study, the two suggested oxidation approaches were studied with tube furnace and muffle furnace given a different result. The study was proved that muffle furnace produces acceptable results than tube furnace. This is attributed to the more precise temperature within the muffle furnace. These results were confirmed by XRD, SEM and FTIR spectrum. The main conclusion indicates that the thermal oxidation followed by rapid cooling lead to a mixed phases of  $\text{CuO}$  and  $\text{Cu}_2\text{O}$  which is dominated by Nano crystals of  $\text{Cu}_2\text{O}$  phase. In addition, UV-Visible absorption spectra exhibits the optical gap of copper oxide nanostructure for all oxidation temperatures found to be 3.6 eV.

## REFERENCES

- [1] Balamurunga B. and Mehta B. R., "Optical and structural properties of nanocrystalline copper oxide thin films prepared by activated reactive evaporation", *SolidThinFilms*(2001) , V396 , issue 1-2,90-96.
- [2] Maurizio M-M, Cristina G., and Emilia G., "Surface-Enhanced Raman Scattering from Copper Nanoparticles Obtained by Laser Ablation", *J. Phys. Chem. C* (2011), 115:5021–5027.
- [3] Mustafa A.H., "Studying the Effect of Doping in Some Physical Properties of Copper Oxide Thin Film", *Eng. and Tech. Journal*, Vol.30, No.14 (2012) pp. 2421-2430.
- [4] Mohammed K. Khalaf, Saba N. Said and Ameen J. Abbas , "Characterization of the Copper Oxide Thin Films Deposited by DC Sputtering Technique" *Eng. and Tech. Journal* , Vol.32 , part (B), No.4 , pp 770-774 (2014).
- [5] Christopher J. L., Smith J.D., Yuehua C. , and Kripa K.V., "Size-dependent thermal oxidation of copper: single-step synthesis of hierarchical nanostructures", *Nanoscale*, (2011), 3, 4972-4976.
- [6] Hassan H. B., and Abdel Hamid Z., "Electrodeposited Cu–CuO Composite Films for Electrochemical Detection of Glucose", *Int. J. Electrochem. Sci.*(2011), 6:5741 – 5758.
- [7] Mohd R.J., Suan M.S.M., Hawan N.L., Hee A.C., "Annealing Effects on the Properties of Copper Oxide Thin Films Prepared by Chemical Deposition", *Int. J. Electrochem. Sci.*(2011), 6:6094 – 6104.
- [8] Haitao Z., Dongxiao H., Zhaoguo M., Daxiong W. A., and Canying Z., "Preparation and thermal conductivity of CuOnanofluid via a wet chemical method", *Nanoscale Research Letters* (2011), 6:181.
- [9] Julia'n M., Luis S., Francisco M., Miguel S., Ramos-Barrado J.R., "Nanostructured CuO thin film electrodes prepared by spray pyrolysis: a simple method for enhancing the electrochemical performance of CuO in lithium cells", *J. Morales et al. / Electrochimica Acta*(2004), 49:4589–4597.
- [10] Yun Q., Jeremy R. E., Ursula M., and Hipps K. W., "Fabrication of graphene with CuO islands by chemical vapor deposition", *Langmuir*(2012), 28 (7):3489-93.
- [11] Santraa K., Sarkara C. K., Mukherjeea M. K., and Ghosh B., "Copper oxide thin films grown by plasma evaporation method", *Thin Solid Films*(1992),213(2):226–229.
- [12] Mugwang'a F. K., Karimi P. K., Njoroge W. K., Omayio O, and Waita S.M., "Optical characterization of Copper Oxide thin films prepared by reactive dc magnetron sputtering for solar cell applications", *Int. J. Thin Film Sci. Tec.*(2013), 2 (1), 15-24.
- [13] Ogwu A., Darma T. H., and Bouquere E., "Electrical resistivity of copper oxide thin films prepared by reactive magnetron sputtering", *Journal of Achievements in Materials and Manufacturing Engineering*(2007), 24 (1):172-174.
- [14] Papadimitropoulos G., Vourdas N., Vamvakas V.M., and Davazoglou D., "Deposition and characterization of copper oxide thin films", *Journal of Physics: Conference Series*, (2005), 10:182–185.
- [15] Gevorkyan V. A., Reymers A. E., Nersesyan M. N., and M A Arzakantsyan M.A., "Characterization of Cu<sub>2</sub>O thin films prepared by evaporation of CuO powder", *Journal of Physics: Conference*(2012), Series 350.
- [16] Lupan O., Pauport'e T., Chow L., Viana B., Pelle F., Ono L.K., and Cuenya B.R., Heinrich H., "Effects of annealing on properties of ZnO thin films prepared by electrochemical deposition in chloride medium", *Applied Surface Science*(2010),256 (6):1895–1907.
- [17] Jenkins R., and Snyder R., "Introduction to X-Ray Powder Diffractometry", *John Wiley & Sons*, New York (2012), 544.
- [18] Kooti M., and Matouri L., "Fabrication of nanosized cuprous oxide using fehling's solution", *Transaction F: Nanotechnology* (2010), 17(1):73-78.

- [19] Mageshwari K., and Sathyamoorthy R., "Flower-shaped CuO Nanostructures: Synthesis, Charecterization and Antimicrobial Activity", *J.Mater. Sci.Technol.*, (2013), 29(10):909-91417.
- [20] Mayur V., Shefaly M., Angshuman P., and Sonal T., "Synthesis and anti-bacterial activity of Cu, Ag and Cu-Ag alloy nanoparticles: A green approach", *Materials Research Bulletin* (2011), 46:384-389.
- [21] Baban C., Rusu G.I., and Prepelita P., "On the optical properties of polycrystalline CdSe thin films," *Journal of Optoelectronics and Advanced Materials*, Vol. 7, No. 2, 817-821, 2005.
- [22] Swarup K.M., Nillohit M., Anup M., Bibhutoh A., and Basudeb K., "Chemical synthesis of mesoporous CuO from a single precursor: Structural, optical and electrical properties", *Journal of Solid State Chemistry* (2010), 183:1900-1904.
- [23] Liang C., Mingwang S., Dayan C., and Yuzhong Z., "Preparation, characterization, and electrochemical application of mesoporous copper oxide", *Materials Research Bulletin* (2010), 45:235-239.
- [24] Singh S. C., Swarnkar R. K, and Gopal R., "Zn/ZnO core/shell nanoparticles synthesized by laser ablation in aqueous environment: Optical and structural characterizations", *Bull. Mater. Sci.* (2010), 33(1): 21-26.
- [25] Bouvy C., and Suy B. L., ZnO@Porous Media, Their PL and Laser Effect, *J. Mater. Sci. Technol.* (2008), 24(4):495-511.